

The behavior of subgrid-scale models near the turbulent/nonturbulent interface in jets

Carlos B. da Silva^{a)}

IDMEC/IST, Technical University of Lisbon, Pav. Mecânica I, 1º andar, Av. Rovisco Pais, 1049-001 Lisboa, Portugal

(Received 27 May 2009; accepted 22 July 2009; published online 10 August 2009)

The behavior of subgrid-scale models near the turbulent/nonturbulent interface in jets is analyzed by using direct numerical simulation and large-eddy simulation (LES). The subgrid scales of motion near this region are far from equilibrium and contain an important fraction of the total kinetic energy. The Smagorinsky constant C_S needs to be corrected near the jet edge and the method used to obtain the dynamic Smagorinsky constant C_D is not able to cope with the intermittent nature of this region. *A priori* tests and LES show that near the jet edge the Smagorinsky model is superior both to the dynamic Smagorinsky and to the gradient models. © 2009 American Institute of Physics. [DOI: 10.1063/1.3204229]

In many free shear flows such as mixing layers, wakes, or jets, a turbulent/nonturbulent (T/NT) interface separates the turbulent (T) and the irrotational (or nonturbulent—NT) flow regions.¹ The T/NT interface is sharp and is continually deformed over a wide range of scales. Important exchanges of mass, momentum, and scalar quantities take place across this interface in a process described as *turbulent entrainment*.² Due to its importance in many engineering and geophysical flows, the physics of the turbulent entrainment has been investigated in many works; however, many details of this process remain today largely unknown.² Recent works showed that the turbulent entrainment appears to be caused by small scale “nibbling” eddy motions instead of by the large-scale “engulfing” mechanism.^{3,4}

This raises new modeling problems in the frame of large-eddy simulation (LES) since in LES the large scales of motion are explicitly computed, while the effect of the small unresolved scales is modeled by a subgrid-scale (SGS) model.⁵ It is well known that important velocity fluctuations exist in the irrotational flow region near the T/NT interface and that these generate important Reynolds stresses near the jet edge.^{1,2,6} Arguably, the details of the entrainment mechanism near the T/NT interface will not affect the entrainment rate, which is thought to be dictated by the dynamics of the large scales of motion. There are however situations in which the details of the small scale nibbling motions may be important. An example is the mixing of scalars near the edge of a jet. Since the mixing rates are governed by the local velocity fluctuations, there is a concern that a deficient prediction of the Reynolds stresses near the T/NT interface may lead to a deficient modeling of the scalar mixing near the T/NT interface and to inaccurate predictions of the mixing and combustion rates in jets.⁷

The goal of the present work is to analyze the challenges faced by the LES methodology near the T/NT interface in a jet and to assess the performance of several LES models in this region. For this purpose, direct numerical simulation

(DNS) and LES of temporally evolving turbulent plane jets were used. The Navier–Stokes solver employs pseudospectral methods for spatial discretization with $(N_1 \times N_2 \times N_3) = (256 \times 384 \times 256)$ collocation points along the streamwise (x) normal (y) and spanwise (z) directions and a third step Runge–Kutta scheme for temporal advancement. The reference DNS is the same as already used by the author and described in detail in Ref. 8. Extensive validation tests showed that the DNS is representative of a fully developed turbulent plane jet. The self-similar regime is obtained at $T/T_{\text{ref}} = H/(2U_1) \approx 20$, where U_1 and H are the initial velocity and the jet slot width, respectively, and the Reynolds number based on the Taylor microscale λ and on the root mean square of the streamwise velocity u' is equal to $\text{Re}_\lambda = u'\lambda/\nu \approx 120$ across the jet shear layer.

Conditional statistics in relation to the distance from the T/NT interface are used throughout this work. The procedure used to obtain these statistics is similar to the one used in several previous works^{2,4} and is briefly outlined here since it was already described in detail in Ref. 8. The sketch in Fig. 1(a) shows the T/NT interface separating the turbulent and the irrotational flow regions at the upper shear layer of the plane jet. The T/NT interface is defined using the vorticity norm $\Omega = (\Omega_i \Omega_i)^{1/2}$, where $\Omega_i = \nabla \times u_i$ is the vorticity field and the detection threshold is $\Omega = 0.7U_1/H$ as in Refs. 2 and 3. The vorticity surface is indicated by a solid line, while the T/NT interface envelope is represented by dashed lines. The T/NT interface envelope location $Y_I(x)$ is determined using a linear interpolation along the y direction for each one of the N_1 grid points along the x direction in the original coordinate system. A new local coordinate system (y_I) is defined at the interface location and the conditional statistics are made in this local coordinate system. The T/NT interface is at $y_I = 0$, while the irrotational and turbulent regions are defined by $y_I < 0$ and $y_I > 0$, respectively. “Holes” of “ambient fluid” that appear inside the jet are removed from the statistical sample. Notice that here, unlike in Ref. 8, the local coordinate system is always aligned in the y direction. This procedure is used also for the lower shear layer and for each one

^{a)}Electronic mail: carlos.silva@ist.utl.pt.

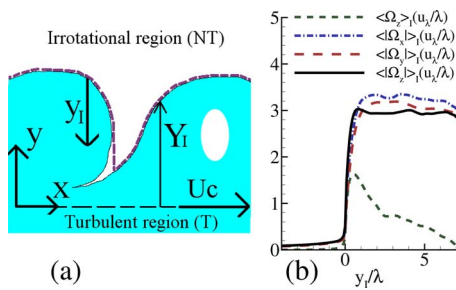


FIG. 1. (Color online) (a) Sketch of the T/NT interface indicating the vorticity surface (solid line) and the interface envelope (dashed lines) with the coordinate system of the plane jet (x, y) and the one used in the conditional statistics in relation to the distance from the T/NT interface (y_I). The interface envelope position is denoted by Y_I and the “hole” represents a region of irrotational fluid inside the turbulent region. (b) Mean conditional profiles of $\langle |\Omega_x| \rangle_I$, $\langle |\Omega_y| \rangle_I$, $\langle |\Omega_z| \rangle_I$, and $\langle \Omega_z \rangle_I$.

of the existing (x, y) planes and the final result is averaged over all these N_3 planes. Finally, to improve the degree of convergence of the statistics $N_T=11$ instantaneous fields taken from the fully developed turbulent regime were also used. We denote these conditional statistics by $\langle \rangle_I$, whereas $\langle \rangle_y$ denotes the classical statistics computed using spatial averaging over the (x, z) planes.

Figure 1(b) shows conditional mean profiles of $\langle |\Omega_x| \rangle_I$, $\langle |\Omega_y| \rangle_I$, $\langle |\Omega_z| \rangle_I$, and $\langle \Omega_z \rangle_I$ in relation to the distance from the T/NT interface nondimensionalized by u_λ/λ , where λ and u_λ are the Taylor microscale and velocity-scale associated with the Taylor scale, respectively, inside the turbulent region, i.e., $u_\lambda = (\varepsilon\lambda)^{1/3}$, where $\varepsilon = 2\nu S_{ij}S_{ij}$ is the viscous dissipation rate. In agreement with other numerical and experimental works,^{4,7} all the vorticity components display a sharp jump at the T/NT interface and the thickness of this jump is roughly equal to the Taylor microscale.

The reference DNS is used to assess *a priori* tests the performance of three SGS models.⁵ The models analyzed here are the Smagorinsky model with $C_S=0.16$, the dynamic Smagorinsky (with the constant C_D computed with plane averaging and clipping to ensure $C_D \geq 0$), and the gradient or nonlinear model with $C_A=1/12$. The separation between grid and subgrid scales is made using a box filter. Filtered variables are denoted by an overbar, e.g., $\tau_{ij} = \overline{u_i u_j} - \overline{u_i} \overline{u_j}$ is the SGS stress tensor and three filter widths were used: $\Delta/\lambda = 0.4, 0.8, 1.6$. The filter size $\Delta/\lambda = 0.4$ is “placed” at the start of the dissipation range, while $\Delta/\lambda = 0.8$ is at the inertial range. $\Delta/\lambda = 1.6$ represents a coarse grid as often used in industrial or geophysical applications.

Figure 2(a) gives a first impression of the challenge faced by LES near the edge of a free shear flow such as the plane jet used here. Conditional profiles of $\langle \tau_{ii} \rangle_I / \langle \overline{u_i} \overline{u_i} \rangle_I$ are displayed in Fig. 2(a). As expected $\langle \tau_{ii} \rangle_I / \langle \overline{u_i} \overline{u_i} \rangle_I$ increases with the filter size. In classical LES the SGS kinetic energy $\tau_{ii}/2$ is always much smaller than the resolved kinetic energy $\overline{u_i} \overline{u_i}/2$. Typical values for the ratio between the two quantities are $\tau_{ii}/\overline{u_i} \overline{u_i} \approx 10\% - 15\%$. Figure 2(a) shows that well into the turbulent region at $y_I/\lambda = 6$, we have indeed $\langle \tau_{ii} \rangle_I / \langle \overline{u_i} \overline{u_i} \rangle_I$ close to 0.10 for the inertial range filter size. However, as one approaches the T/NT interface $\langle \tau_{ii} \rangle_I / \langle \overline{u_i} \overline{u_i} \rangle_I$

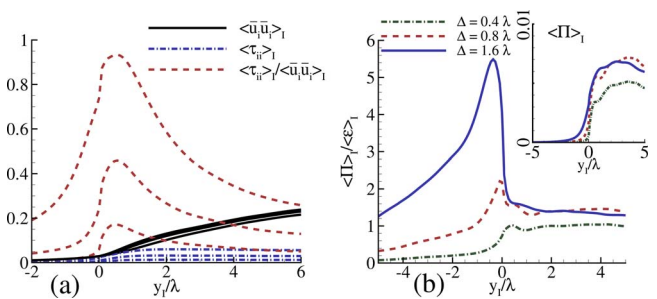


FIG. 2. (Color online) Conditional profiles of SGS related quantities for filter widths $\Delta/\lambda = 0.4, 0.8, 1.6$. (a) Ratio between the SGS and the grid-scale kinetic energy $\tau_{ii}/\overline{u_i} \overline{u_i}$. (b) Ratio between the SGS energy production $\Pi = -\tau_{ij} S_{ij}$ and the viscous dissipation rate $\varepsilon = 2\nu S_{ij} S_{ij}$. The inset shows the conditional profile of the SGS energy production Π .

increases and attains extremely high values which are untypical of LES: $\langle \tau_{ii} \rangle_I / \langle \overline{u_i} \overline{u_i} \rangle_I \approx 0.45$ at $y_I/\lambda = 0.5$ for $\Delta/\lambda = 0.8$ (inertial range). The DNS showed that as expected $\tau_{ii} \rightarrow 0$ as $y_I \rightarrow -\infty$.

As part of the turbulent entrainment mechanism, fluid elements from the irrotational flow region must acquire kinetic energy as they approach the T/NT interface.⁶ Therefore, one might be tempted to suggest that the turbulent entrainment is a process dominated by backward energy transfer (backscatter), as in the early stages of transition in a jet. The inset in Fig. 2(b) shows conditional profiles of SGS kinetic energy production $\Pi = -\tau_{ij} S_{ij}$, where $S_{ij} = \frac{1}{2}(\partial \overline{u_i} / \partial x_j + \partial \overline{u_j} / \partial x_i)$ is the resolved rate-of-strain tensor. $\Pi > 0$ implies a forward energy transfer from grid to subgrid scales (backscatter occurs whenever $\Pi < 0$). The inset in Fig. 2(b) shows that inside the irrotational flow region $\langle \Pi \rangle_I$ is close to zero but remains always positive, and it acquires a roughly constant value in the turbulent zone after a sharp jump near the T/NT interface. Thus, the overall effect of the entrainment is one of mean forward scatter of kinetic energy from the large to small scales of motion, which shows a fundamental difference between the transition stages of a jet and the transition to turbulence that takes place across the T/NT interface. In order to fully understand what detailed mechanisms lay behind the generation of SGS energy close to the T/NT interface, the SGS kinetic energy transport equation should be investigated.

Another interesting result is related to the balance between the production of SGS kinetic energy Π , and the viscous dissipation rate $\varepsilon = 2\nu S_{ij} S_{ij}$. It is well known that Π and ε do not balance locally, i.e., the “local equilibrium assumption” which is implicitly used in many SGS models does not hold.⁹ However a “global equilibrium” is observed in most turbulent flows $\langle \Pi \rangle / \langle \varepsilon \rangle \approx 1$. Figure 2(b) shows that this is not the case near the T/NT interface. In particular, inside the irrotational region close to the T/NT interface at $y_I/\lambda \leq -1$ the subgrid scales are far from equilibrium. This shows that the interaction between grid and subgrid scales near the T/NT interface is more involved than in fully developed turbulence.

In order to assess the behavior of the SGS models near the T/NT interface we compare the model constants for each model with their “correct” value given by the DNS.^{5,10} For

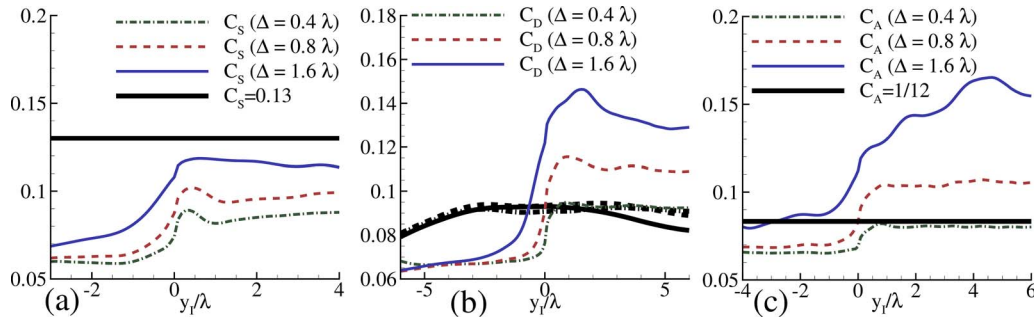


FIG. 3. (Color online) Conditional profiles of SGS model constants for $\Delta/\lambda=0.4, 0.8, 1.6$. (a) Smagorinsky constant C_S . (b) Dynamic Smagorinsky constant C_D . Thin colored lines correspond to $\langle C_D \rangle_I$, whereas the thick dark lines represent conditional profiles of C_D based on the $\langle C_D \rangle_y$ with the classical plane averaging procedure. (c) Gradient model constant C_A .

the Smagorinsky model the constant C_S is calculated through $\langle C_S^2 \rangle_I = \langle -\tau_{ij} \overline{S_{ij}} \rangle_I / \langle 2\Delta^2 |\overline{S}| \overline{S_{mn}} \overline{S_{mn}} \rangle_I$. Figure 3(a) shows the conditional mean profile of C_S for several filter widths. In isotropic turbulence by invoking local equilibrium and an inertial range energy spectrum, $C_S = 1/\pi(2/3C_k) = 0.16$ is obtained for a Kolmogorov constant equal to $C_k = 1.6$. In free shear flows the optimal value is $C_S = 0.13$ and it is this value that is shown for reference in Fig. 3(a). The conditional mean profile of C_S shows that inside the turbulent region $y_l/\lambda = 4$ we have $C_S \approx 0.10$, which is smaller than the classical value of $C_S = 0.16$ but agrees with numerous numerical and experimental works.^{5,10} However, close to the T/NT interface, C_S decreases and attains $C_S \approx 0.062 - 0.075$, thus suggesting that the classical value of C_S if used may inhibit the growth of the Reynolds stresses near the T/NT interface.^{1,6}

Using the results from Phillips¹ the asymptotic behavior of several SGS quantities can be obtained inside the irrotational flow region for $y_l < -L_{11}$, where L_{11} is the integral scale $L_{11} = \int_0^\infty f(r) dr$ and $f(r) = \langle u(x+r)u(x) \rangle_I / \langle u^2(x) \rangle_I$ is the longitudinal correlation function. Notice that in the irrotational flow region the energy spectrum does not display a $-5/3$ inertial range. Instead, it exhibits a rapid fall off in the high wave number region, as the distance to the T/NT interface increases.⁶ Consequently $|\overline{S}| \approx |S|$, where $|S| = (2S_{ij}S_{ij})^{1/2}$ is the rate-of-strain norm. The results from Ref. 1 imply that the viscous dissipation rate evolves as $\varepsilon \sim -y_l^{-6}$, which gives $|\overline{S}| \sim -y_l^{-3}$.

The asymptotic law for the turbulent eddy viscosity can be obtained by considering a filter size equal to the Taylor microscale $\Delta \approx \lambda$, which is representative of a good LES, and by using another result from Ref. 1 ($\lambda \sim -y_l$). The turbulent eddy viscosity evolves as $\nu_T \sim \Delta^2 |\overline{S}| \sim -y_l^{-1}$. This decay law is recovered in the present DNS for y_l/λ far away from the T/NT interface. The SGS kinetic energy evolves as $\tau_{ii} \sim (\nu_T/\Delta)^2 \sim -y_l^{-4}$ and, therefore, the power law for the SGS kinetic energy production is $\Pi \sim \tau_{ii} |\overline{S}| \sim -y_l^{-7}$, and $\Pi/\varepsilon \sim -y_l^{-1}$ in agreement with the present results for $\Delta/\lambda = 0.8$.

The asymptotic law for the correct value of C_S is $C_S \sim (\tau_{ii} |\overline{S}| / \Delta^2 |\overline{S}|^3)^{1/2} \sim -y_l^0$, which shows that a constant value should be recovered. Figure 3(a) shows that this value is $C_S \approx 0.06$ for $\Delta/\lambda = 0.8$, which is substantially smaller than the classical values for isotropic turbulence or free shear

flows. This value is close however to $C_S = 0.065$, which has been used in channel flows.⁵

It is interesting to discuss one important difference between the eddy viscosity in LES and in Reynolds averaged Navier–Stokes simulations (RANS), which is denoted here by ν_T^{RANS} . In SGS models based on the eddy viscosity assumption, this quantity is defined through $\tau_{ij} - (1/3)\delta_{ij}\tau_{kk} = -2\nu_T S_{ij}$, where τ_{ij} is the SGS stress tensor, whereas in RANS the eddy viscosity is defined as $\langle u'_i u'_j \rangle - (1/3)\delta_{ij}\langle u'_i u'_i \rangle = -2\nu_T^{\text{RANS}} \langle S_{ij} \rangle$, where $\langle u'_i u'_j \rangle$ is the Reynolds stress tensor and $\langle S_{ij} \rangle$ is the mean rate-of-strain tensor.

Using the $k-\varepsilon$ model, the eddy viscosity is given by $\nu_T^{\text{RANS}} = C_\mu k^2 / \varepsilon$, where $k = \langle u'_i u'_i \rangle / 2$ (C_μ is a model constant) and at the irrotational region this model is ill-defined because $\varepsilon \rightarrow 0$. One way to overcome this difficulty is to set the eddy viscosity ν_T^{RANS} equal to a constant inside the irrotational region.¹¹ LES based in, e.g., the Smagorinsky model do not suffer from this limitation because as shown in Ref. 8 ε (and therefore also $|\overline{S}|$) tends to zero in the irrotational region which means that $\nu_T(\vec{x}, t) = (C_S \Delta)^2 |\overline{S}| \rightarrow 0$ as $y_l \rightarrow -\infty$.

Figure 3(b) shows the conditional profiles of the dynamic Smagorinsky constant C_D using the classical procedure involving plane averaging in the (x, z) plane $\langle C_D \rangle_y = \langle L_{ij} M_{ij} \rangle_y / \langle M_{mn} M_{mn} \rangle_y$ and using the conditional averaging procedure $\langle C_D \rangle_I = \langle L_{ij} M_{ij} \rangle_I / \langle M_{mn} M_{mn} \rangle_I$, where $L_{ij} = \widehat{\widehat{u_i u_j}} - \widehat{u_i} \widehat{u_j}$ is the Leonard stress tensor defined with $\hat{\Delta} = 2\Delta$, and $M_{ij} = -2\Delta^2 (2|\widehat{S}| \widehat{S}_{ij} - |\widehat{S}| \widehat{S}_{ij})$. The conditional dynamic constant $\langle C_D \rangle_I$ changes quite abruptly across the T/NT interface displaying $\langle C_D \rangle_I \approx 0.11 - 0.13$ for $y_l/\lambda > 0$ and $\langle C_D \rangle_I \approx 0.065$ for $y_l/\lambda < 0$. The values found for C_D inside the turbulent region agree with several previous works.¹⁰ However, the classical procedure gives $\langle C_D \rangle_y \approx 0.08 - 0.09$ near the T/NT interface $-6 < y_l/\lambda < +6$. This shows that the classical procedure is not able to distinguish between turbulent and irrotational flow and, consequently, “mixes” information from both regions, leading to a decrease in the average value of C_D near the T/NT interface. This might lead to an over-prediction of the Reynolds stresses near the T/NT interface in LES. Finally, by comparing the model constants C_S and C_D we see that $C_D \approx 0.09$ is always smaller than $C_S = 0.16$ which shows that the dynamic Smagorinsky model is less dissipa-

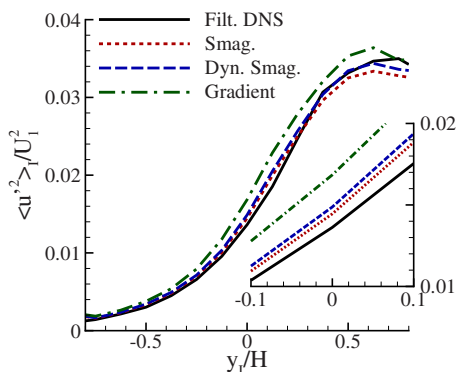


FIG. 4. (Color online) Conditional streamwise Reynolds stress $\langle u'^2 \rangle_I$ from LES with $(32 \times 48 \times 32)$ grid points using the Smagorinsky model (Smag), dynamic Smagorinsky (dyn Smag), and gradient models. The conditional Reynolds stress $\langle u'^2 \rangle_I$ from the filtered DNS (filt DNS) is also shown for comparison and the inset highlights the region near the T/NT interface.

tive than the Smagorinsky model both inside the irrotational and the turbulent regions.

The model constant C_A was computed by equating the “real” and modeled SGS energy production II. The results displayed in Fig. 3(c) show that for $\Delta/\lambda=0.8$ the model constant C_A is roughly constant and slightly higher than the theoretical value of $C_A=1/12$ inside the turbulent region $\langle C_A \rangle_I \approx 0.11$ for $y_I/\lambda > 0$ but falls to a constant inside the irrotational region $\langle C_A \rangle_I \approx 0.07$ for $y_I/\lambda < 0$.

Starting from the filtered DNS fields at the self-similar region several LES of plane jets were carried out with the three models. Several grid sizes were used with $N_i^{\text{LES}} = N_i/\beta$, $i=1,2,3$ and $\beta=2,4,8,16$ corresponding to an implicit filter size of $\Delta/\lambda=0.2,0.4,0.8,1.6$. All the simulations were run from $T/T_{\text{ref}} \approx 20$ to 25. Figure 4 shows the conditional Reynolds stresses $\langle u'^2 \rangle_I$ from the LES with $\beta=8$ and the result from the filtered DNS. In agreement with Ref. 2, the irrotational Reynolds stresses are very important near the T/NT interface attaining $\langle u'^2 \rangle_I / U_1^2 \approx 0.014$ at $y_I/H=0$ which is about half of the value inside the fully developed turbulent region $\langle u'^2 \rangle_I / U_1^2 \approx 0.034$. As expected from numerous studies,⁵ inside the turbulent region $y_I/H > 0.3$ and compared to the filtered DNS values the Smagorinsky model is too dissipative, the gradient model does not dissipate enough energy, while the best results are obtained with the dynamic Smagorinsky model. Near the T/NT interface $-0.3 < y_I/H < 0.3$ the Smagorinsky model is more dissipative than the dynamic Smagorinsky model and the gradient model is the least dissipative model. Taking the filtered DNS as the correct behavior, we conclude that the Smagorinsky model gives better results than the dynamic model near the T/NT interface of the jet. Similar results were obtained in the other simulations.

The effects of the SGS models on the shear layer growth

rate can be assessed by comparing the jet half-widths $\delta_{0.5}$ from the LES at the same instant. The observed differences are very small (about 1%), which can in part be explained by the relatively small temporal extent of the LES but agrees with the prevailing idea according to which the *entrainment rate is imposed by the large-scale motions*, which are fully resolved in LES, though it “acts” at the small scales. Nevertheless, the results show that $\delta_{0.5}^{\text{Smag}} < \delta_{0.5}^{\text{dyn Smag}} < \delta_{0.5}^{\text{grad}}$, which is consistent with the observed Reynolds stresses near the T/NT interface, i.e., the gradient model spreads faster due to its higher Reynolds stresses near the interface. Arguably, mixing and reaction rates near the interface should be more affected.

The present results clearly show that the classical SGS models are unable to cope with the strong inhomogeneity of the flow near jet edge. The sharp T/NT interface is generated by the presence of nearby intense vorticity structures,^{12,13} and a detailed understanding of their effects on the interface can be used to develop corrections to the classical SGS models near the T/NT interface. Future work will focus on the development of corrective measures for the SGS models based on the available theory.^{1,6}

¹O. M. Phillips, “The irrotational motion outside a free turbulent boundary,” *Proc. Cambridge Philos. Soc.* **51**, 220 (1955).

²D. K. Bisset, J. C. R. Hunt, and M. M. Rogers, “The turbulent/nonturbulent interface bounding a far wake,” *J. Fluid Mech.* **451**, 383 (2002).

³J. Mathew and A. Basu, “Some characteristics of entrainment at a cylindrical turbulent boundary,” *Phys. Fluids* **14**, 2065 (2002).

⁴J. Westerweel, C. Fukushima, J. M. Pedersen, and J. C. R. Hunt, “Mechanics of the turbulent-nonturbulent interface of a jet,” *Phys. Rev. Lett.* **95**, 174501 (2005).

⁵C. Meneveau and J. Katz, “Scale invariance and turbulence models for large-eddy simulation,” *Annu. Rev. Fluid Mech.* **32**, 1 (2000).

⁶D. J. Carruthers and J. C. R. Hunt, “Velocity fluctuations near an interface between a turbulent region and a stably stratified layer,” *J. Fluid Mech.* **165**, 475 (1986).

⁷J. Mellado, L. Wang, and N. Peters, “Gradient trajectory analysis of a scalar field with external intermittency,” *J. Fluid Mech.* **626**, 333 (2009).

⁸C. B. da Silva and J. C. F. Pereira, “Invariants of the velocity-gradient, rate-of-strain, and rate-of-rotation tensors across the turbulent/nonturbulent interface in jets,” *Phys. Fluids* **20**, 055101 (2008).

⁹C. B. da Silva and J. C. F. Pereira, “On the local equilibrium of the subgrid-scales: The velocity and scalar fields,” *Phys. Fluids* **17**, 108103 (2005).

¹⁰H. S. Kang and C. Meneveau, “Experimental study of an active grid-generated mixing layer and comparisons with large-eddy simulation,” *Phys. Fluids* **20**, 125102 (2008).

¹¹J. B. Cazalbou, P. R. Spalart, and P. Bradshaw, “On the behavior of two-equation models at the edge of a turbulent region,” *Phys. Fluids* **6**, 1797 (1994).

¹²J. C. R. Hunt, I. Eames, and J. Westerweel, “Vortical interactions with interfacial shear layers,” in *Proceedings of IUTAM Conference on Computational Physics and New Perspectives in Turbulence*, Nagoya, September 2006, edited by Y. Kaneda (Springer Science, Berlin, 2008).

¹³J. C. R. Hunt, I. Eames, and J. Westerweel, “Eddy dynamics near sharp interfaces and in straining flows,” in *Proceedings of European Conference on Mathematics in Industry*, July 2008 (Springer, Berlin, 2009).